Cell Reports
Physical Science

CellPress

Supplemental Information for

Gripping, Catching, and Conveying with a Soft, Toroidal Hydrostat

Samuel E. Root,[1,2] Daniel J. Preston,[1] Gideon O. Feifke,[1] Hunter Wallace,[1] Renz Marion Alcoran,[1] Markus P. Nemitz,[1] Jovanna A. Tracz,[1] and George M. Whiteside*[1]

[1]Department of Chemistry and Chemical Biology, Harvard University, 12 Oxford Street, Cambridge, MA 02138, USA
[2]Lead Contact
*Correspondence: gmwhitesides@gmwgroup.harvard.edu

Cell Reports
Physical Science

CellPress

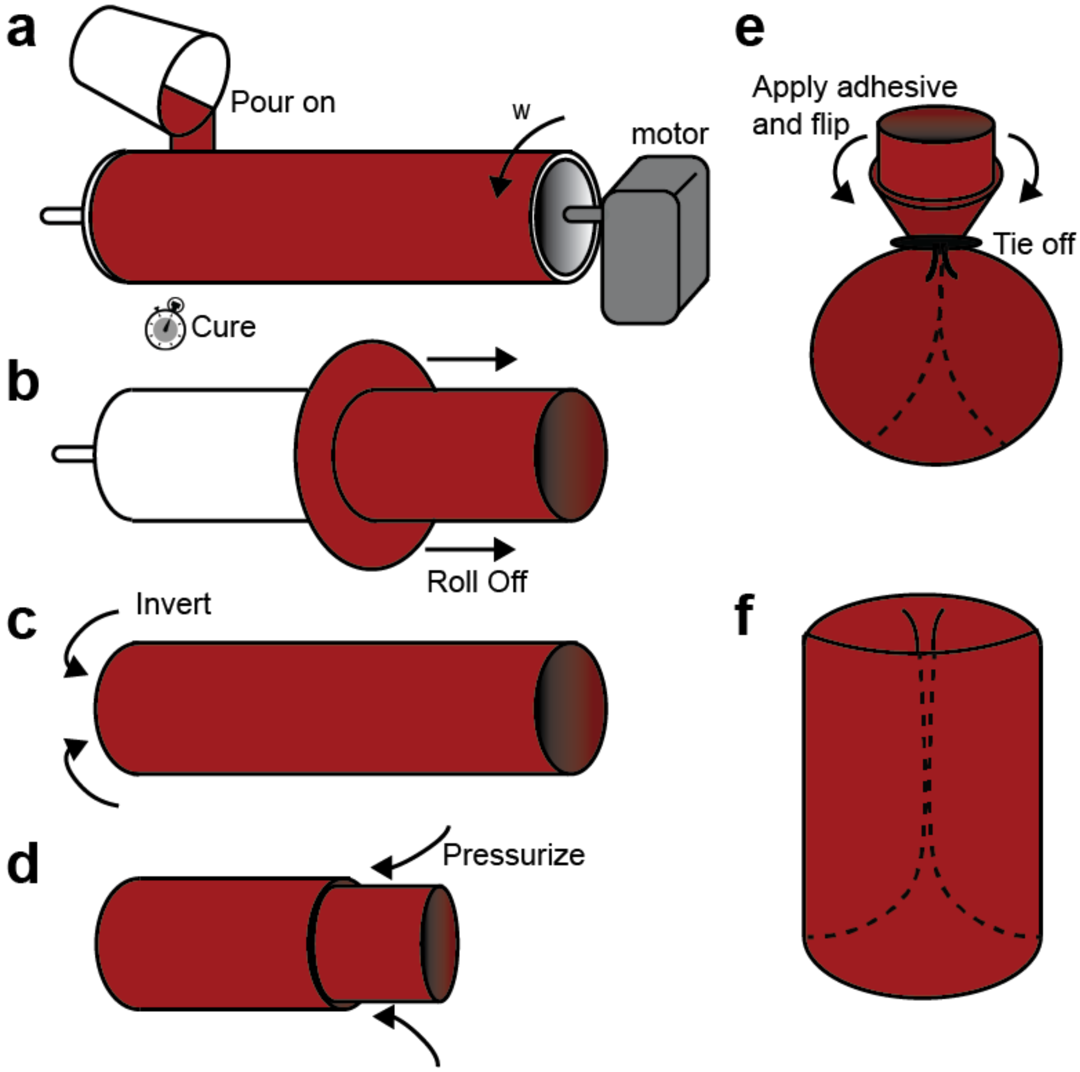

Figure S1. Fabrication of a silicone toroidal hydrostat.
(a) Silicone pre-polymer is cast onto a rotating PVC pipe. (b) Once cured, the tube is rolled off and (c) inverted manually. (d) The inverted tube is then pressurized with water from a sink and tied off with a rubber band. (e) Adhesive is applied and the toroid is sealed off. (f) The string is untied, resulting in a pressurized toroidal hydrostat.

Cell Reports
Physical Science

Figure S2. Photograph of an air-filled toroidal hydrostat containing a Schrader valve.
Shown with the valve facing outwards (left) and inwards (right).

Cell Reports
Physical Science

CellPress

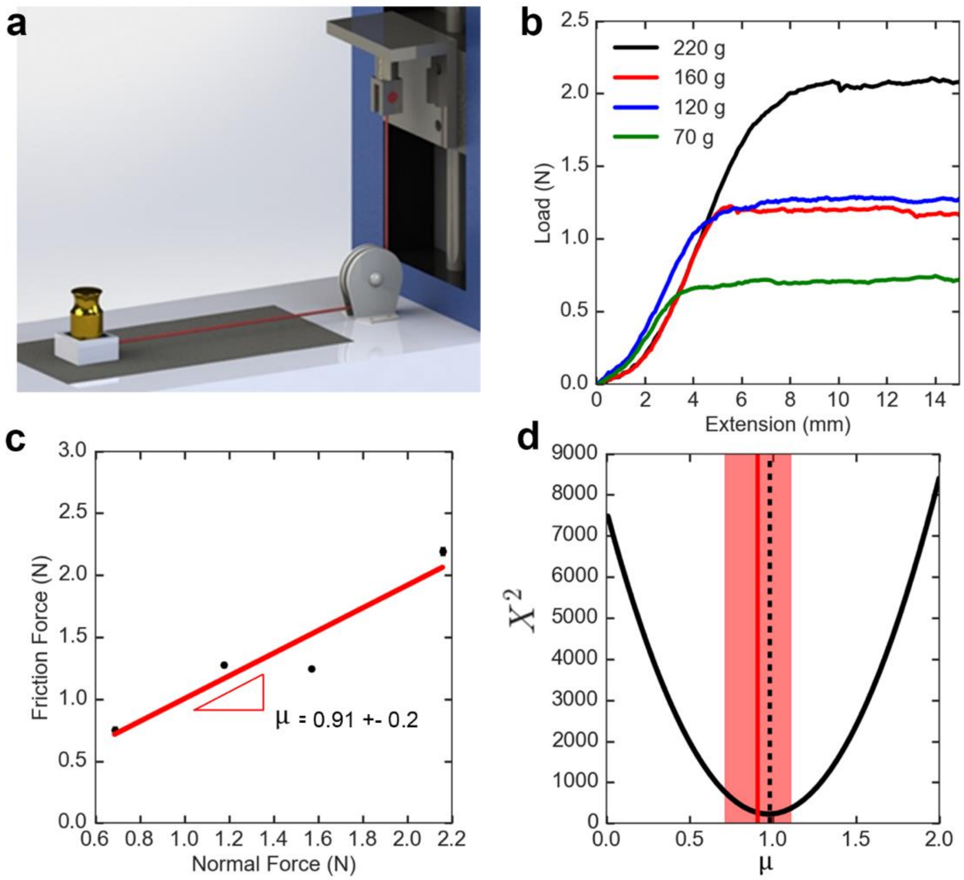

Figure S3. Measurements of coefficient of friction.

(a) Computer rendering of experimental setup for measuring the coefficient of friction. A sled was attached to an Instron using a pulley system to apply a tangential load. (b) Load versus extension plots obtained from friction sled experiments. The force of friction was taken from the plateaued regions of the plots. (c) Plot of friction force versus normal force used to calculate the coefficient of friction via linear regression. (d) Plot showing relationship between the independently measured coefficient of friction (vertical red line) and the value obtained by using the coefficient of friction as a fitting parameter for our cylindrical gripping model (vertical dashed black line.) The shaded red region indicates the standard error from the linear regression to the friction sled measurements.

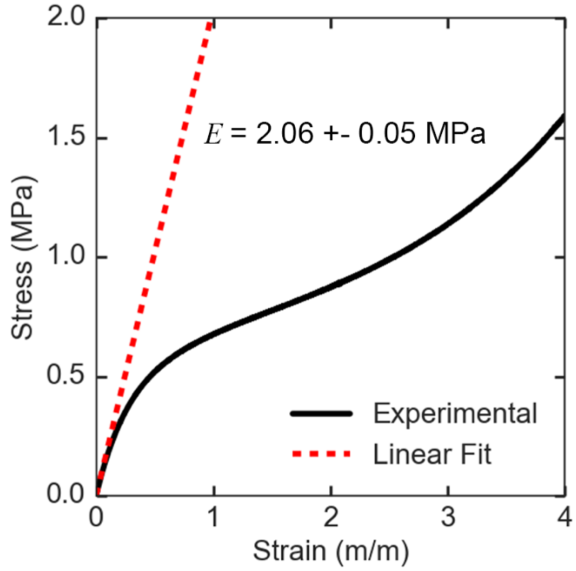

Figure S4. Stress strain curve of thermoplastic elastomer membrane.
Obtained from pull-testing (50 mm/min) a section of the elastomeric membrane from the commercially available 'water wiggly.' The elastic modulus was calculated by fitting a 10th-order polynomial to the entire curve and then taking the derivative at zero strain to obtain the linear fit shown by the dashed red line. Average value and standard deviation for the modulus were obtained from 7 independent experiments.

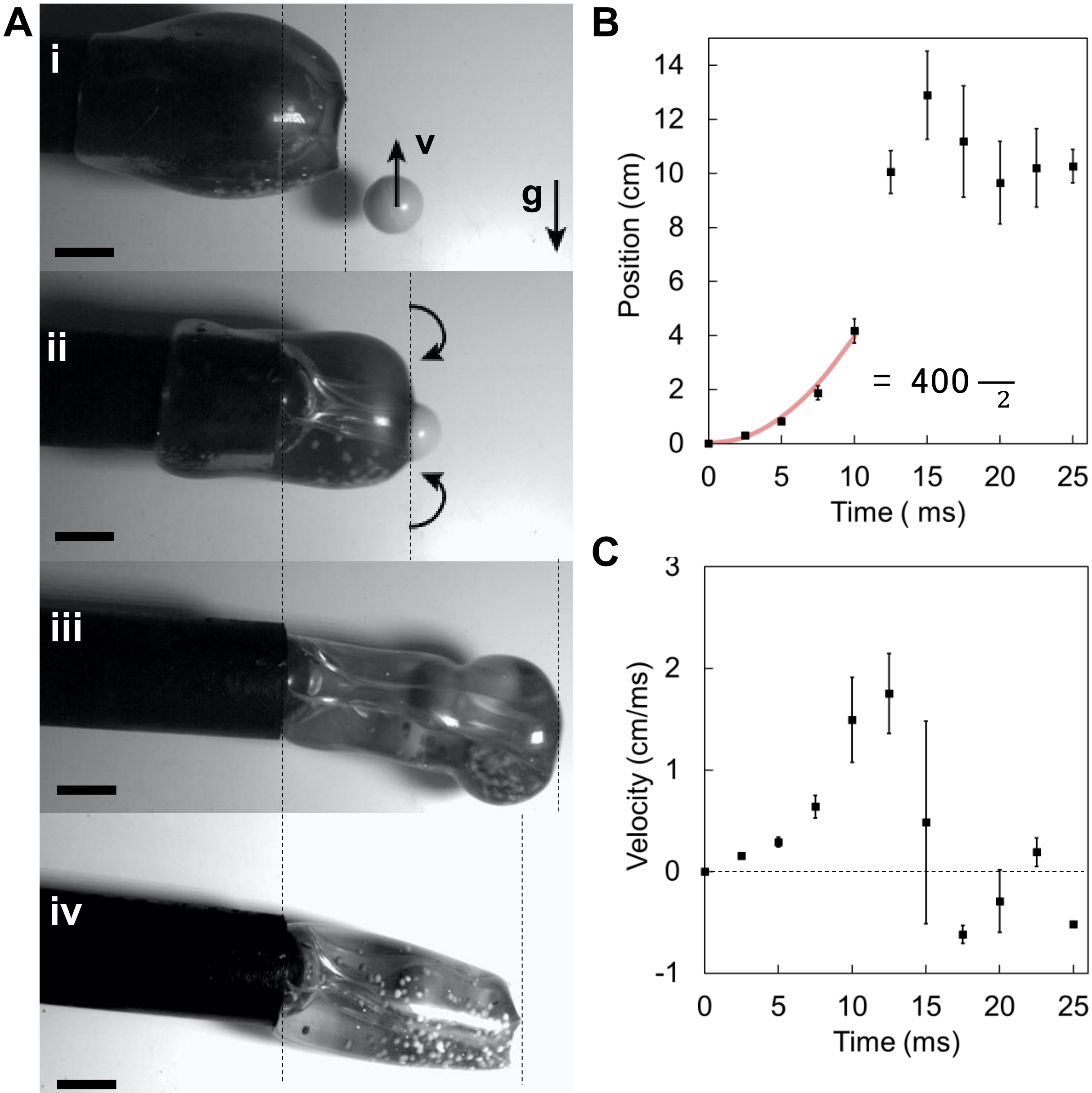

Figure S5. (A) Images of the catching process obtained from a high-speed camera (Phantom V7.1). (B) A plot of position of the tip of the toroid versus time used to infer the acceleration of the process by fitting to a quadratic model. (C) A plot of velocity versus time obtained by numerical differentiation of the position versus time data.

Cell Reports
Physical Science

Supplementary Notes

Note S1. Derivation of Hydrostatic Gripping Model

The toroidal hydrostat exerts a frictional gripping force. Coulomb's approximate model for dry friction states that:

$$F_C \leq \mu F_n , \quad \text{eq. (S1)}$$

where F_C is the fiction force, μ is the static coefficient of friction and F_n is the normal force. For the case of a hydrostatic gripper:

$$F_n = PA_o , \quad \text{eq. (S2)}$$

where P is the hydrostatic pressure and A_O is the area of the object in contact with the hydrostat. Additionally, the incompressible nature of water in the hydrostat implies the following conservation of volume relation:

$$V_H = V_{H0} + V_r + V_o , \quad \text{eq. (S3)}$$

where V_i (for $i = H, H0, r, o$) are the volumes of the hydrostat, the unperturbed hydrostat, the rod and the object respectively. For the case of a cylindrical rod and object (**Figure 3a**), equation (S3) produces the following relation:

$$R_H = \sqrt{R_{H0}^2 + \frac{l_p}{l_H} R_p^2 + \frac{l_o}{l_H} R_o^2} , \quad \text{eq. (S4)}$$

where l_i, R_i (for $i = H, H0, r, o$) are the length and radius of the hydrostat, the unperturbed hydrostat, the rod, and the object respectively. The average circumferential strain in the membrane, ε can be approximated as:

$$\varepsilon \approx \frac{R_H - R_i}{R_i} . \quad \text{eq. (S5)}$$

Where R_i is the initial radius of the elastomeric tube before it has been pressurized and sealed off. Assuming a linear elastic response, the circumferential stress, σ, in the membrane is:

$$\sigma = E\varepsilon , \quad \text{eq. (S6)}$$

where E is the tensile modulus of the membrane, which was measured to be 2 MPa. For a thin membrane in a cylindrical geometry, the circumferential stress can be related to the internal pressure by the Young-Laplace equation:

$$P = \frac{\sigma t}{R_H} , \quad \text{eq. (S7)}$$

where t is the thickness of the membrane in the stretched state. Assuming a Poisson's ratio of ν = 0.5, t is related to the undeformed thickness of membrane, t_o, by:

$$\frac{t}{t_0} = \frac{R_i}{R_H}, \quad \text{eq. (S8)}$$

The dimensionless critical gripping force predicted from our model is obtained by combining equations S1-8 and can be written as:

$$\frac{F_C}{E t_0 R_i} = 2\pi\mu R_o l_o \left(\frac{1}{R_i R_H} - \frac{1}{R_H^2}\right) . \quad \text{eq. (S9)}$$

Cell Reports
Physical Science

CellPress

Note S2. Fitting of Model to Experimental Data

A 3x4 matrix was constructed to represent the experimentally measured critical gripping force, F_{ij}^{exp}, as a two-dimensional function of the independent variables l_o/l_H and R_o/R_i. Equation (S10) was fit to this dataset by finding the value of μ that minimized the following residual formula:

$$\chi^{2}(\mu) = \sum_{i=1}^{3}\sum_{j=1}^{4}\frac{\left(F_{ij}^{exp} - F_{ij}^{model}(\mu)\right)^{2}}{\sigma_{ij}^{2}}, \qquad \text{eq. (S10)}$$

where $F_{ij}^{model}(\mu)$ is the model prediction for a given value of μ, and σ_{ij}^{2} is the variance matrix describing the uncertainty of the measurements. The results are displayed in **Figure S3d**.